Biochimie 167 (2019) 135–144

Contents lists available at ScienceDirect

Biochimie

journal homepage: www.elsevier.com/locate/biochi

Research paper

Babesia divergens glycosylphosphatidylinositols modulate blood coagulation and induce Th2-biased cytokine profiles in antigen presenting cells

Françoise Debierre-Grockiego [a, 1, *], Terry K. Smith [b, 1], Stéphane Delbecq [c], Céline Ducournau [a], Louis Lantier [a], Jörg Schmidt [d], Virginie Brès [c], Isabelle Dimier-Poisson [a], Ralph T. Schwarz [d, e, 2], Emmanuel Cornillot [f, g, 2]

[a] ISP, Université Tours, INRA, 37000, Tours, France
[b] Biomedical Sciences Research Complex, University of St Andrews, St Andrews, Fife, Scotland, KY16 9ST, UK
[c] Vaccination Antiparasitaire, Université de Montpellier, 34093, Montpellier, France
[d] Institut für Virologie, AG Parasitologie, Philipps-Universität Marburg, 35043, Marburg, Germany
[e] Univ. Lille, CNRS, UMR 8576, Unité de Glycobiologie Structurale et Fonctionnelle, 59655, Villeneuve d'Ascq, France
[f] Institut de Biologie Computationnelle, 34095, Montpellier, France
[g] Institut de Recherche en Cancérologie de Montpellier (IRCM – INSERM U1194), Institut Régional du Cancer de Montpellier (ICM), Université de Montpellier, 34095, Montpellier, France

ARTICLE INFO

Article history:
Received 2 January 2019
Accepted 29 January 2019
Available online 1 October 2019

Keywords:
Antigen presentation
Coagulation
Glycosylphosphatidylinositol
Interleukin
Major histocompatibility complex

ABSTRACT

Glycosylphosphatidylinositols (GPIs) are glycolipids described as toxins of protozoan parasites due to their inflammatory properties in mammalian hosts characterized by the production of interleukin (IL)-1, IL-12 and tumor necrosis factor (TNF)-α. In the present work, we studied the cytokines produced by antigen presenting cells in response to ten different GPI species extracted from *Babesia divergens*, responsible for babesiosis. Interestingly, *B. divergens* GPIs induced the production of anti-inflammatory cytokines (IL-2, IL-5) and of the regulatory cytokine IL-10 by macrophages and dendritic cells. In contrast to all protozoan GPIs studied until now, GPIs from *B. divergens* did not stimulate the production of TNF-α and IL-12, leading to a unique Th1/Th2 profile. Analysis of the carbohydrate composition of the *B. divergens* GPIs indicated that the di-mannose structure was different from the evolutionary conserved tri-mannose structure, which might explain the particular cytokine profile they induce. Expression of major histocompatibility complex (MHC) molecules on dendritic cells and apoptosis of mouse peritoneal cells were also analysed. *B. divergens* GPIs did not change expression of MHC class I, but decreased expression of MHC class II at the cell surface, while GPIs slightly increased the percentages of apoptotic cells. During pathogenesis of babesiosis, the inflammation-coagulation auto-amplification loop can lead to thrombosis and the effect of GPIs on coagulation parameters was investigated. Incubation of *B. divergens* GPIs with rat plasma *ex vivo* led to increase of fibrinogen levels and to prolonged activated partial thromboplastin time, suggesting a direct modulation of the extrinsic coagulation pathway by GPIs.

1. Introduction

Babesiosis caused by *Babesia divergens*, a protozoan parasite of the *Apicomplexa* phylum transmitted by the *Ixodes ricinus* tick, is an emerging disease in both human beings and animals [1]. Symptomatic patients present malaria-like febrile illness, but as babesiosis can be asymptomatic, it represents a major transfusion threat [2–4]. Only two standard antimicrobial combinations currently exist to treat human babesiosis: atovaquone and azithromycin,

Abbreviations: APTT, Activated partial thromboplastin time; AT, Antithrombin; PECs, Peritoneal exudate cells; PT, Prothrombin time; SRDC, Sophie Ruiz dendritic cells; TAT, Thrombin-antithrombin; TLR, Toll-like receptor.

* Corresponding author. BioMédicaments Anti-Parasitaires, Faculté de Pharmacie, 37200, Tours, France.
E-mail address: francoise.debierre@univ-tours.fr (F. Debierre-Grockiego).

[1] These authors contributed equally to this work and are co-first authors.
[2] These authors contributed equally to this work and are co-last authors.

https://doi.org/10.1016/j.biochi.2019.09.007

effective and well tolerated, or clindamycin and quinine, especially useful in severe cases, but unfortunately poorly tolerated [1]. Erythrocyte exchange apheresis is required to complete the treatment [5].

During pathogenesis due to *B. divergens*, progression of the inflammation-coagulation auto-amplification loop leads to thrombosis, ischemia and in some rare cases, to death [6]. This might be due to Disseminated Intravascular Coagulation syndrome, an imbalance in haemostasis defined by an elevation of procoagulant factors (thrombin-antithrombin [TAT] and fibrin) and a decrease in antithrombin levels, as observed in dogs naturally infected with *B. canis* [7]. In animals experimentally infected with *B. canis*, both activated partial thromboplastin time (APTT) and level of fibrinogen in plasma increased in correlation with lower number of platelets [8].

Regulation of pro-inflammatory Th1 and anti-inflammatory Th2 cytokine production by *Babesia* has been studied *in vitro* and *in vivo*. *B. bovis* merozoites (extracellular form) increased NO production and IL-1β, IL-12p40, TNF-α and IL-10 mRNA expression in bovine monocytes, but not in dendritic cells [9]. IFN-γ, but no IL-10 was produced by blood mononuclear cells from *B. divergens*-infected sheep stimulated *in vitro* with merozoite protein extract [10]. High levels of the regulatory cytokine IL-10 were detected in the serum of *B. microti*-infected mice and of *B. rossi*-infected dogs [11,12]. In *B. microti*-infected mice, the progressive fall in parasitemia from peak values at 14 days post infection was inversely proportional to the rise of IL-10 and parasite-specific IgG production, suggesting a role for IL-10-linked antibody responses in the reduction and clearance of the parasite [13].

To determine which parasite fraction is able to stimulate cells, a membrane-enriched fraction of *B. bovis* merozoites or supernatants from *B. bovis*-stimulated $CD4^+$ T-cell lines containing IFN-γ and TNF-α have been tested on bovine macrophages and both induced production of NO, partially responsible for parasite replication inhibition and phagocytosis of infected erythrocytes *in vitro* [14,15]. Phosphatidic acid from a *B. bovis* attenuated strain and the combination of phosphatidylserine-phosphatidylinositol from attenuated and virulent strains were able to increase Th1 (TNF-α, IL-6), but not Th2 (IL-4) and regulatory (IL-10) cytokine production by mouse peritoneal macrophages in a TLR (Toll-Like Receptor)2-dependent pathway [16]. Glycosylphosphatidylinositols (GPIs) are abundant glycolipids in the membranes of all apicomplexan parasites. GPIs have been determined as parasite toxins participating in pathogeny due to their pro-inflammatory properties [17]. In the present study, we have investigated the role of *B. divergens* GPIs in the modulation of antigen presenting cells in terms of cytokine production, major histocompatibility molecule expression and apoptosis. In addition, direct effect of GPIs on the regulation of the coagulation system was explored *ex vivo*.

2. Materials and methods

2.1. Metabolic labelling of B. divergens GPIs

Merozoites of *B. divergens* strain Rouen 1987 were maintained *in vitro* in human erythrocytes (5% packed cell volume in Roswell Park Memorial Institute [RPMI] 1640 medium with 10% human serum). Metabolic labelling of *B. divergens* was performed in 20 mL glucose-free RPMI 1640 medium (Sigma) supplemented with 20 mM fructose, 25 mM Hepes and 0.5 mCi D-[6-^{3}H]-glucosamine hydrochloride (Hartmann Analytic GmbH) for 4 h at 37 °C. After centrifugation, erythrocytes were lysed with a solution of NaCl at 0.2%, neutralized by the addition of same volume of NaCl at 1.6%. After centrifugation, the pellet was frozen at −80 °C and washed in phosphate buffered saline (PBS). This step permitted the merozoites to detach from residual erythrocyte membranes. Glycolipids of free merozoites were extracted with chloroform-methanol-water (10:10:3, by volume) by sonication (ultrasound bath Branson 3200, 47 MHz) and recovered in the *n*-butyl alcohol phase after partitioning between water-saturated *n*-butyl alcohol and water (1:1, by volume) by centrifugation. Samples were separated by TLC on Silica Gel 60 plate (Merck) using a chloroform-methanol-water (4:4:1, by volume) solvent system. Silica plates were scanned for radioactivity using a Berthold LB 2842 linear analyser.

2.2. Purification of individual GPIs of B. divergens

Large amounts (1×10^{10}) of non-labelled merozoites were collected and GPIs not linked to proteins were extracted with chloroform-methanol-water (10:10:3, by volume) by sonication, dried under a nitrogen stream and recovered in the *n*-butyl alcohol phase after partitioning between water-saturated *n*-butyl alcohol and water (1:1, by volume) by centrifugation. GPIs were precipitated under a stream of nitrogen to remove contaminating phospholipids [18]. GPIs were then separated by TLC on 0.5 mm silica gel 60 plate (Merck, GPIs from 5×10^9 parasites/plate) using a chloroform-methanol-water (4:4:1, by volume) solvent system, with spots of labelled GPIs used as tracers. TLC plates were scanned for radioactivity using a Berthold LB 2842 linear analyser and areas corresponding to individual GPIs were scraped off the plate, re-extracted with chloroform-methanol-water (10:10:3, by volume) by sonication (only half of the material is estimated to be recovered) and residual silica was removed by water-saturated *n*-butyl alcohol/water partition. GPIs were stored at −20 °C in *n*-butyl alcohol until use. Absence of endotoxin in each GPI was checked with the Pierce® *Limulus* Amebocyte Lysate Chromogenic Endotoxin Quantitation kit according to the manufacturer's instructions (Thermo Scientific).

2.3. Quantification and composition analysis of carbohydrates of B. divergens GPIs

The method is based upon quantification of the GlcN residues of the GPIs being converted to Man_3-anhydromannitol (AHM) as described elsewhere [19].

2.4. Composition analysis of phosphatidylinositol moieties of B. divergens GPIs

Individual *B. divergens* GPIs were dried and dissolved in sodium acetate followed by the addition of sodium nitrite. The PI moieties released by deamination were partitioned into *n*-butyl alcohol. The *n*-butyl alcohol extracts were dried, suspended in chloroform-methanol and analysed by negative ion electrospray mass spectrometry (ES-MS, ABsciex 4000 QTrap). Daughter ion ES-MS-MS spectra were obtained with a collision voltage of 35–50 V [20].

2.5. Cell stimulation and cytokine/SEAP activity quantification

Antigen presenting cells were seeded at 2×10^5 in 96-well plates in 100 μL Dulbecco's Modified Eagle Medium (DMEM) for RAW 264.7 macrophage cell line (ATCC® TIB-71™), at 10^6 in 24-well plates in 300 μL DMEM for peritoneal exudates cells (PECs) harvested from Swiss OF1 mice by washing with 5 mL DMEM (directive 2010/63/EU not applied [chapter 1, article 1.5.]) and at 10^6 in 24-well plates in 300 μL RPMI for SRDC dendritic cell line (Applied Biological Materials Inc.). HEK-Blue™ hTLR2 and hTLR4 cells (InvivoGen) were seeded at 2×10^5 in 96-well plates in 100 μL DMEM/1% fetal calf serum without selection antibiotics. The cells

were stimulated at 37 °C in 5% CO_2 atmosphere for 24 h with individual GPIs purified from 5×10^8 (10^8 for HEK-Blue™ cells) merozoites of *B. divergens* or with 200 ng/mL of lipopolysaccharide (LPS from *Escherichia coli* serotype 055:B5, Sigma). The amount of GPIs needed for one experiment was dried under a nitrogen stream to remove the solvent *n*-butyl alcohol. GPIs were suspended in culture medium (in 100 or 300 μL/well for RAW 264.7 and HEK-Blue™ or PECs and SRDC, respectively) by sonication. For the negative control, cells were incubated with same volume of *n*-butyl alcohol dried and suspended in medium by sonication. Levels of cytokines were quantified in the cell culture supernatants by using specific sandwich enzyme-linked immunosorbent assay (ELISA) from Affymetrix eBioscience or MACSPlex Cytokine 10 Kit, mouse from Miltenyi Biotec GmbH, following the manufacturer's instructions. SEAP (secreted embryonic alkaline phosphatase) reporter gene activity of HEK-Blue™ cells was measured at 630 nm after addition of QUANTI-Blue™ detection medium (InvivoGen) to supernatant.

2.6. Measurement of MHC expression and apoptosis

SRDC and PECs were stimulated as described above (2.5.). Supernatant was centrifuged at 300×*g* to pool floating cells and attached cells after their detachment using accutase (Affymetrix eBioscience). After centrifugation at 300×*g*, supernatant was removed for quantification of cytokines (section 2.5.) and pelleted SRDC were suspended and saturated for 30 min on ice in PBS containing 1% bovine serum albumin, 2% mouse serum and 0.1% azide (PBS-BSA-azide). After centrifugation, 3×10^5 SRDC were incubated for 30 min on ice in the dark in PBS-BSA-azide with 0.5 μg fluorescein isothiocyanate (FITC) mouse anti-mouse H−2K [k] MHC class I antibody (clone 36-7-5, BD Pharmingen™), 0.5 μg FITC mouse anti-mouse I-E[k] MHC class II antibody (clone 14-4-4S, BD Pharmingen™), or 0.5 μg FITC mouse IgG2a, κ isotype control (clone G155-178, BD Pharmingen™). After centrifugation, SRDC were suspended in 300 μL PBS-2% paraformaldehyde and analysed by flow cytometry (BD FACSCalibur™ and CellQuest™ software, BD Bioscience). PECs were incubated for 15 min at 4 °C in the dark in 100 μL binding buffer (10 mM Hepes pH 7.4, 140 mM NaCl, 5 mM $CaCl_2$) with 5 μL annexin V-FITC (BD Pharmingen™) and 5 μg/mL propidium iodide (Sigma). After centrifugation, PECs were suspended in 300 μL binding buffer and analysed by flow cytometry.

2.7. Measurement of coagulation parameters

Blood was taken from non-infected adult male Wistar rat anesthetized with 60 mg/kg pentobarbital. Nine volumes were mixed with one volume of trisodium citrate at 0.109 M (32%). Plasma was separated by centrifugation during 15 min at 2500×*g*. Half of the plasma sample was incubated for 30 min at room temperature with GPIs of *B. divergens* (from 5×10^8 merozoites for 200 μL plasma). Before adding GPIs, the solvent *n*-butyl alcohol was dried under a nitrogen stream and GPIs were suspended in 10 μL of Owren-koller buffer by sonication. Half of the plasma sample was incubated for 30 min at room temperature with 10 μL of Owren-koller buffer containing dried *n*-butyl alcohol alone. Negative and positive controls of coagulation, all reagents and Star 4 coagulation analyser were from Stago (France). Fibrinogen level was measured on sample diluted at 1/10 and 1/20 (final volume of 100 μL) with Fibri-Prest® Automate 2 (thrombin + heparine inhibitor) reagent, PT was measured on 50 μL sample with Neoplastine® CI Plus (thromboplastin + calcium) reagent and APTT was measured on 50 μL sample with C.K. Prest® (cephalin + kaolin activator) or Cephascreen® (cephalin + polyphenol activator) reagent, according to the manufacturer's instructions. All results are expressed in time of coagulation and given in seconds.

2.8. Statistics

The non-parametric one-way ANOVA test followed by the Dunnett's multiple comparison test (for not significantly different variances determined with Bartlett's test), the non-parametric Kruskal-Wallis test or the Friedman test followed by the Dunn's multiple comparison test (for significantly different variances determined with Bartlett's test) and the Wilcoxon test were used for statistical evaluation (GraphPad Prism 7).

3. Results

3.1. Analysis of carbohydrate and lipid composition of B. divergens GPIs

To detect the GPIs of *B. divergens* for the first time, merozoites were metabolically labelled with [^{3}H]-glucosamine during *in vitro* culture within erythrocytes. Merozoites were separated from erythrocyte membrane by osmotic lysis and freezing. After their extraction with organic solvents, the different GPI species were separated by TLC and detected with a Berthold analyser. As shown in Fig. 1, two GPIs (3 and 8) were predominantly labelled, while eight GPIs were less expressed in *B. divergens* merozoites. In order to study biological effects of GPIs on mammalian cells and to determine their carbohydrate and lipid contents, GPIs were extracted from large amounts of merozoites. Contaminant phospholipids were completely eliminated by precipitation of GPIs [18]. After the separation of GPIs on preparative TLC, silica was scraped off according to the full width at half maximum of each peak. By this way, individual GPIs were highly purified. Based upon AHM and inositol quantification, GPI3 was the most abundant GPI species with more than 400−500 $\times 10^4$ copies per merozoite (Table 1). In contrast, GPI10 was the lowest represented GPI species with less than 3×10^4 copies per merozoite. Except for GPI8, quantification was consistent with the counts of radioactivity on Fig. 1. The carbohydrate composition analysis by GC-MS of *B. divergens* GPIs revealed the presence of a maximum of two mannoses (Table 2). Galactose was detected on GPI1 and GPI2, but not on the other GPI species (Table 2). Mass spectroscopy analysis of the PI moieties showed that each GPI species exists in several forms with different fatty acid methyl esters (from 16:0 to 24:0) or diacyls (from 34:1 to

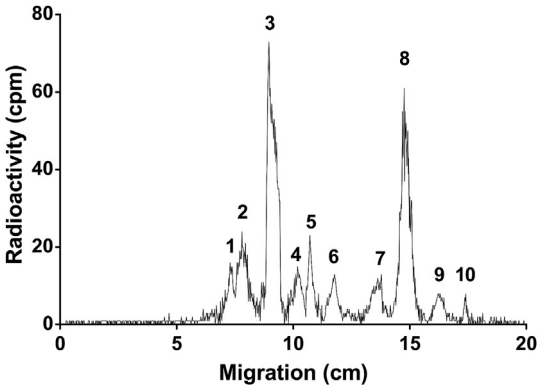

Fig. 1. Detection of metabolically labelled GPIs of *B. divergens*. Merozoites were labelled with D-[6-^{3}H]-glucosamine and GPIs were extracted with chloroform-methanol-water (10:10:3, by volume) followed by partition between water-saturated *n*-butyl alcohol and water (1:1, by volume). GPIs were then separated by TLC using a chloroform-methanol-water (4:4:1, by volume) solvent system and detected by the Berthold analyser.

Table 1
AHM and inositol quantifications of individual GPIs of *B. divergens*.

Sample	GPI1	GPI2	GPI3	GPI4	GPI5	GPI6	GPI7	GPI8	GPI9	GPI10
AHM quantification ($\times 10^4$ copies per cell)	12.3 ± 1.6	39.2 ± 7.1	407.0 ± 18.0	12.1 ± 1.3	9.46 ± 0.49	7.92 ± 0.31	1.90 ± 0.16	4.38 ± 0.16	1.22 ± 0.09	1.07 ± 0.06
Inositol quantification ($\times 10^4$ copies per cell)	1.54 ± 0.17	43.3 ± 6.3	511.0 ± 38.0	18.0 ± 0.9	14.9 ± 1.5	12.0 ± 1.0	2.06 ± 0.07	8.01 ± 0.62	1.44 ± 0.17	2.85 ± 0.38

Each GPI was submitted to base hydrolysis, deamination/reduction, methanolysis and TMS derivatisation for its subsequent analysis by GC-MS.
Single ion monitoring of *m/z* 273 was selected to detect AHM and *m/z* 318 to detect both *scyllo*- and *myo*-inositol.
The peak areas of the corresponding standards were used to calculate the molar relative response, allowing quantification of both AHM and *myo*-inositol in the samples.
Values are means of molar ratios ± standard error of two replicates (equivalent to 2×10^8 parasites, each).
AHM: anhydromannitol.

Table 2
Carbohydrate composition analysis of individual GPIs of *B. divergens*.

Sample	GPI1	GPI2	GPI3	GPI4	GPI5	GPI6	GPI7	GPI8	GPI9	GPI10
Ino	1.0 ± 0.1	1.0 ± 0.1	1.0 ± 0.1	1.0 ± 0.1	1.0 ± 0.1	1.0 ± 0.1	1.0 ± 0.1	1.0 ± 0.1	1.0 ± 0.1	1.0 ± 0.1
Man	**1.9 ± 0.3**	**2.3 ± 0.2**	**2.2 ± 0.2**	**1.9 ± 0.3**	**2.1 ± 0.2**	**1.9 ± 0.3**	1.3 ± 0.2	0.1 ± 0.1	0.1 ± 0.1	0.1 ± 0.1
GlcNAc	1.2 ± 0.2	1.1 ± 0.1	1.3 ± 0.2	1.2 ± 0.2	1.0 ± 0.1	1.2 ± 0.2	1.0 ± 0.1	1.2 ± 0.2	0.9 ± 0.2	1.1 ± 0.1
Gal	**1.7 ± 0.2**	**0.9 ± 0.3**	0.1 ± 0.1	0.1 ± 0.1	0.1 ± 0.1	0.1 ± 0.1	0.1 ± 0.1	0.1 ± 0.1	0.1 ± 0.1	0.1 ± 0.1

Each GPI was submitted to base hydrolysis, deamination/reduction, methanolysis and derivatisation for its analysis by GC-MS.
The peak areas of the corresponding standards were used to calculate the molar relative response, allowing determination of monosaccharide content.
GlcNAc levels were calculated from AHM generated during deamination.
Values are means of molar ratios ± standard error of two replicates.
Ino: inositol; Man: mannose; GlcNAc: *N*-acetyl-glucosamine; Gal: galactose.

48:0) at various ratios (Fig. 2A: ES-MS results for GPI3 and GPI8, Fig. 2B: ES-MS-MS results for GPI3 and GPI10, Table 3: results for all GPI species). Altogether, composition analysis gives the proposed GPI-pathway illustrated in Fig. 3: GlcNAc-PI (GPI9), GlcN-PI (GPI8), GlcN-(acyl)PI (GPI10), Man-GlcN-(acyl)PI (GPI7), Man-Man-GlcN-(acyl)PI (GPI4, GPI5, GPI6, with remodelled long fatty acids), Man-Man-GlcN-PI (GPI3), (Gal)-Man-Man-GlcN-PI (GPI2), (Gal-Gal)-Man-Man-GlcN-PI (GPI1), with GPI8 and GPI3 the major GPI-intermediates. GPI4, GPI5, GPI6, GPI7 and GPI10 had an acylated inositol and the clear 640 m/z fragment ion strongly suggests

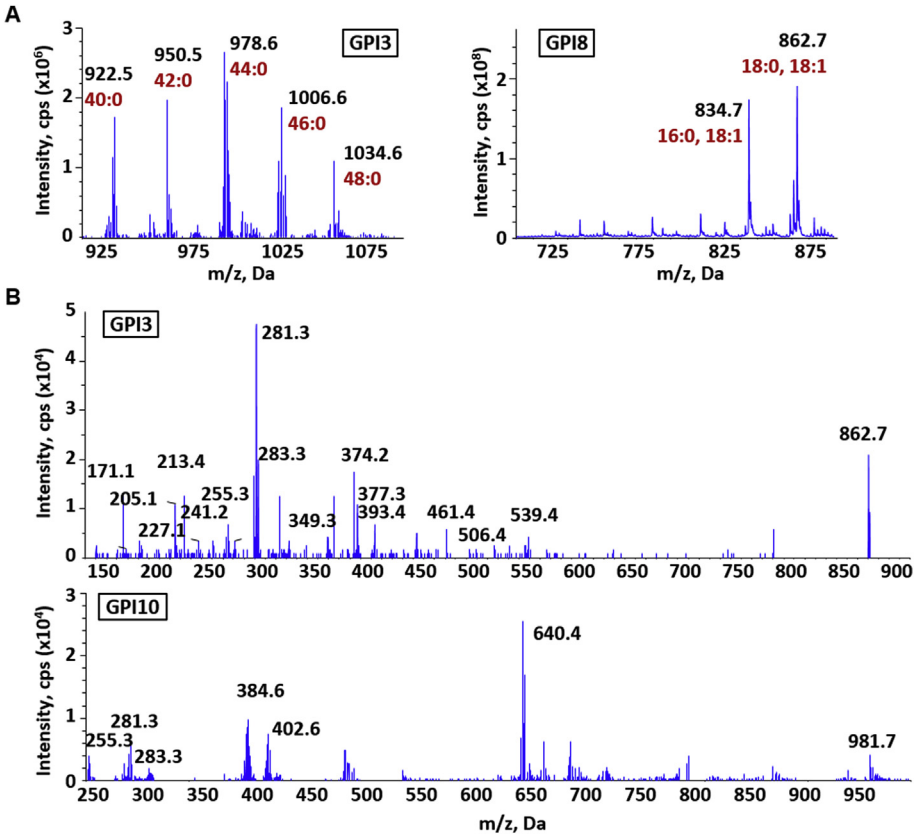

Fig. 2. Spectra of the PI moieties released by deamination from individual *B. divergens* GPIs. ES-MS spectra of the PI moieties from GPI3 and GPI8 (**A**) and ES-MS-MS spectra of the PI moieties from GPI3-863 m/z and GPI10-1262 m/z (**B**): 384.6 m/z = GlcN-inositol-cyclic-phosphate, 402.6 m/z = GlcN-inositol-phosphate, 640.4 m/z = GlcN-(palmitoyl)inositol-phosphate. Fatty acids of all GPI species are listed in Table 3.

Table 3
MS analysis of the PI moieties and their corresponding fatty acid content released by deamination from individual *B. divergens* GPIs.

Sample	GPI1	GPI2	GPI3	GPI4	GPI5	GPI6	GPI7	GPI8	GPI9	GPI10
Observed m/z	NA	922.5	922.5	NA	NA	NA	NA	863	863	1262
		950.5	950.5					835	835	1234
		978.6	978.6							
		1006.6	1006.6							
		1034.6	1034.6							
Diacyl*		40:0	40:0					36:1	36:1	36:1
		42:0	42:0					34:1	34:1	34:1
		44:0	44:0							
		46:0	46:0							
		48:0	48:0							
FAME	24:0 (9)	24:0 (7)	24:0 (7)	18:0 (5)	22:0 (3)	24:0 (4)	18:0 (5)	18:0 (5)	18:0 (7)	18:0 (3)
	22:0 (4)	22:0 (4)	22:0 (4)	18:1 (9)	20:0 (2)	22:0 (3)	18:1 (10)	18:1 (10)	18:1 (10)	18:1 (8)
	20:0 (1)	20:0 (2)	20:0 (2)	16:0 (7)	18:0 (4)	20:0 (2)	16:0 (7)	16:0 (8)	16:0 (6)	16:0 (8)
					18:1 (5)	18:0 (7)				
					16:0 (7)	16:0 (8)				

PI moieties were subjected to base hydrolysis, acidification, extraction and derivatisation prior to analysis of fatty acid methyl ester by GC-MS.
Some of the PI moieties released by deamination were analysed by negative ion ES-MS.
All of the molecular species refer to the corresponding peaks in the negative ion mode in Fig. 2. Observed [M − H]-ions, mass over charge from survey scans as described in the experimental procedure section.
*Peak identities refer to total number of carbon atoms and double bonds.
NA: not analysed.
FAME: fatty acid methyl ester (values in parenthesis are the ratio of FAME).

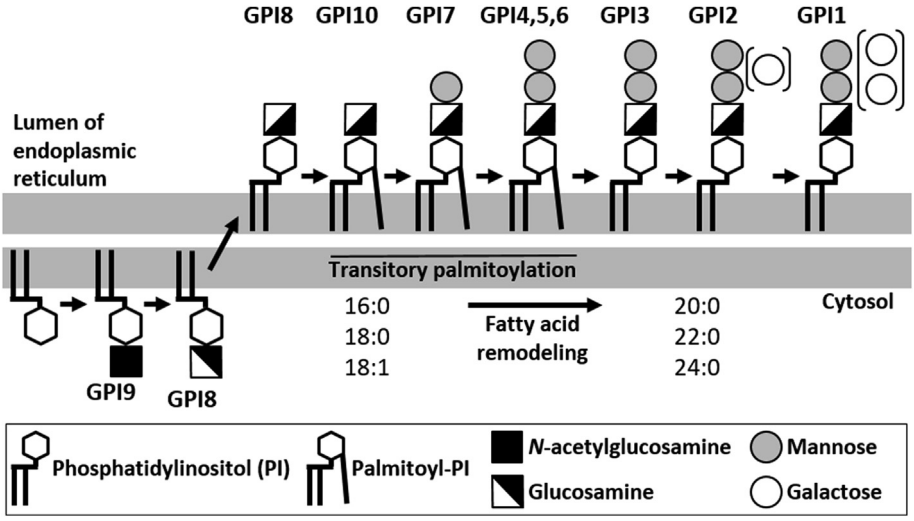

Fig. 3. Hypothetical pathway of GPI biosynthesis in *B. divergens*. GPI biosynthesis starts at the cytoplasmic leaflet of the reticulum endoplasmic membrane with the transfer of *N*-acetyl-glucosamine to phosphatidylinositol (PI) to give phosphatidylinositol-*N*-acetyl-glucosamine (GPI9), followed by the de-N-acetylation to give phosphatidylinositol-glucosamine (GPI8). After transfer to the luminal side of the endoplasmic reticulum, palmitoylation of the inositol ring takes place to give GlcN-(acyl)PI (GPI10). Then, addition of two successive mannoses and fatty acid remodelling give Man-GlcN-(acyl)PI (GPI7) and Man-Man-GlcN-(acyl)PI (GPI4, GPI5, GPI6). Inositol depalmitoylation leads to Man-Man-GlcN-PI (GPI3). Finally, galactose is added leading to (Gal)-Man-Man-GlcN-PI (GPI2) and (Gal-Gal)-Man-Man-GlcN-PI (GPI1).

exclusive palmitoylation on the inositol, as there was no fragment ion at either 612 or 668 m/z, which would correspond to myristoyl or stearoyl, respectively (GPI10 spectra on Fig. 2B).

3.2. Responses of antigen presenting cells to B. divergens GPIs

3.2.1. Production of cytokines

In order to study the role of *B. divergens* GPIs in cytokine production, macrophages and dendritic cells were stimulated *in vitro*. For this, macrophages of the RAW 264.7 cell line, non-elicited peritoneal exudate cells (PECs, rich in macrophages), or dendritic cells of the SRDC cell line were stimulated during 24 h with the ten individual GPIs extracted from 5×10^8 merozoites of *B. divergens* and cytokine levels were quantified in the cell culture supernatant by sandwich ELISA. *B. divergens* GPIs induced the production of the anti-inflammatory cytokines IL-5 and the regulatory cytokine IL-10 (Fig. 4). The range of produced cytokines was different between the three cell types and varied according to the GPI species. After their stimulation with *B. divergens* GPIs, PECs produced significantly higher levels of IL-5 (Fig. 4A upper histogram, $p = 0.003$ Kruskal-Wallis test), but not of IL-10 (Fig. 4A lower histogram, $p = 0.109$ Kruskal-Wallis test) compared to the control condition, certainly due to important variation. In the presence of *B. divergens* GPIs, RAW 264.7 macrophages showed the lowest increases in IL-5 levels (Fig. 4B upper histogram, $p = 0.015$ one-way ANOVA test), but the most significant global increase in IL-10 levels (Fig. 4B lower histogram, $p = 0.0003$ Kruskal-Wallis test). Increases of IL-5 levels produced by SRDC in response to the GPIs were highly significant (Fig. 4C upper histogram, $p = 0.0001$ Kruskal-Wallis test), while increases of IL-10 production by this cell type were modest (Fig. 4C lower histogram, $p = 0.0196$ Kruskal-Wallis test). Regarding individual GPIs, PECs were significantly stimulated by GPI7 to GPI10 to

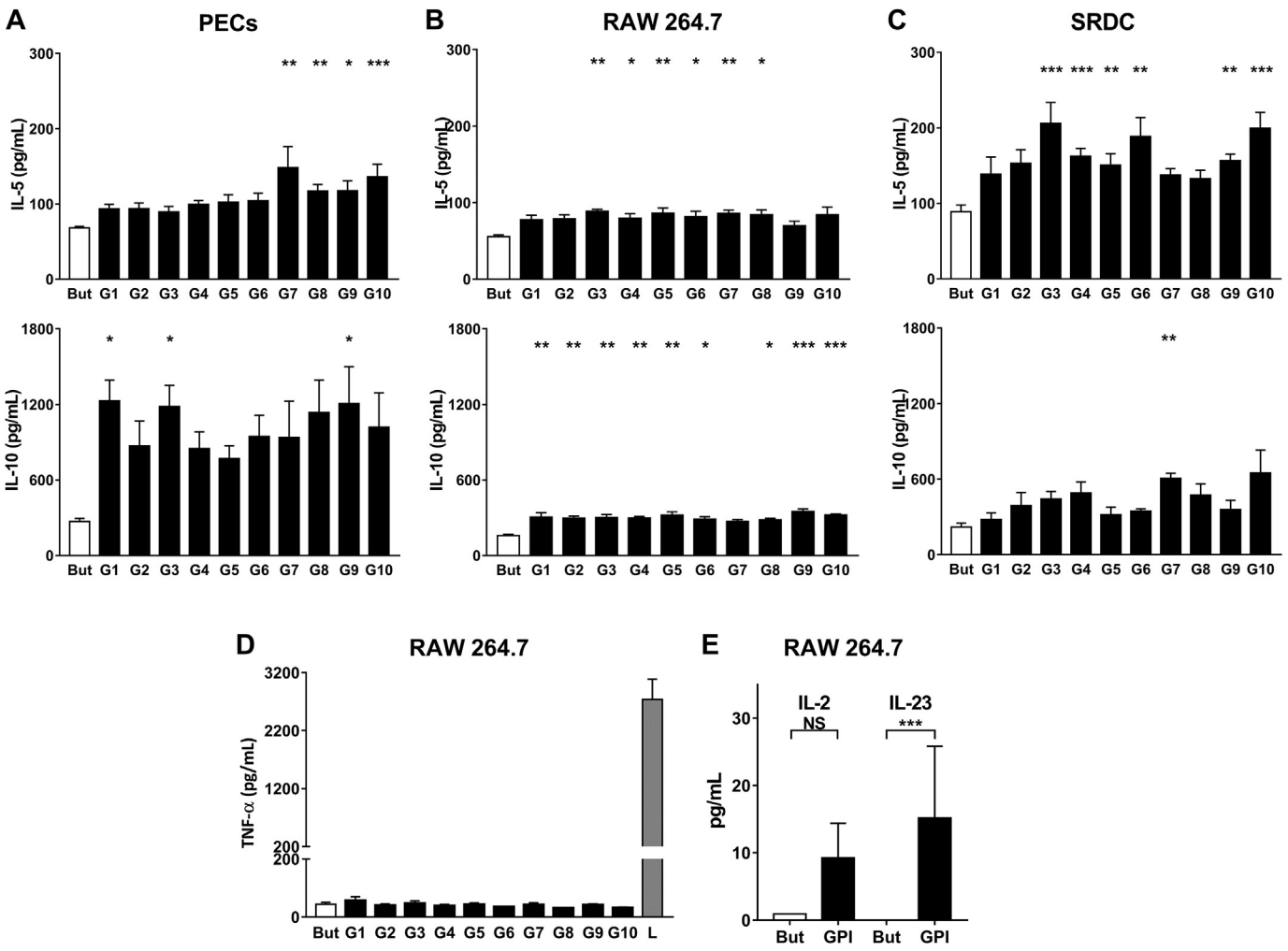

Fig. 4. Cytokine production by antigen presenting cells in response to GPIs of *B. divergens*. RAW 264.7 macrophages (**A**), peritoneal exudate cells (**B**) and SRDC dendritic cells (**C**) were stimulated for 24 h with the ten individual GPIs (G1 to G10) purified from 5×10^8 merozoites of *B. divergens* or with dried solvent *n*-butyl-alcohol (But) as negative control. IL-5 and IL-10 were quantified in supernatant by sandwich ELISA. Results are mean +SEM (standard error of the mean) with n = 6 or 9. Histograms are representative of 2–6 independent experiments; $^{*}p < 0.05$, $^{**}p < 0.01$, $^{***}p < 0.001$ (Bartlett's test for IL-5 production by RAW 264.7; Dunn's multiple comparison test for other results). TNF-α levels were quantified in supernatant of RAW 264.7 macrophages by sandwich ELISA (**D**). Results are mean +SEM with n = 5. IL-2 and IL-23 were quantified by MACSPlex kit in supernatant of RAW 264.7 macrophages (**E**). Results are mean +SEM of the 10 individual GPIs; $^{***}p < 0.001$ (Dunn's multiple comparison test).

produce IL-5 and by GPI1, GPI3 and GPI9 to produce IL-10; RAW 264.7 macrophages were significantly stimulated by GPI3 to GPI8 to produce IL-5 and by all GPIs except GPI7 to produce IL-10; SRDC were significantly stimulated by GPI3 to GPI6, GPI9 and GPI10 to produce IL-5 and by GPI7 to produce IL-10 (Figs. 4A, B, C). Similar levels of IL-5 and IL-10 were obtained with higher amounts of GPIs (data not shown). In contrast to GPIs of other protozoan parasites studied until now, GPIs of *B. divergens* did not enhance the production of IL-1β, IL-12 and TNF-α by any of the cells tested, whereas bacterial lipopolysaccharide used as positive control did (IL-1β: 35.1 ± 1.7 pg/mL with butanol, from 30.4 ± 1.6 to 34.3 ± 1.7 pg/mL with GPIs, 128.1 ± 1.7 pg/mL with LPS; IL-12: 1.9 ± 2.8 pg/mL with butanol, from 1.7 ± 0.6 to 5.5 ± 1.2 pg/mL with GPIs, 51.7 ± 2.3 pg/mL with LPS; TNF-α: Fig. 4D). To further characterise the cytokine profile induced by *B. divergens* GPIs, a larger panel of cytokines was quantified by flow cytometry in the supernatant of RAW 264.7 macrophages. Levels of IFN-γ (Th1), IL-4 (Th2), GM-CSF and IL-17A (Th17) were under the detection threshold (data not shown). Compared to the control condition, the GPIs induced very low levels of IL-2, but significantly higher levels of IL-23, representative of a Th17 profile (Fig. 4E). Altogether, these results showed that the GPIs of *B. divergens* orientate antigen presenting cells towards a unique Th1/Th2/Th17 profile compared to the pro-inflammatory profile induced by GPIs of all other protozoan parasites explored until now.

3.2.2. TLR signalling

To determine whether *B. divergens* GPIs are ligands of TLRs, HEK293T cells modified to express alkaline phosphatase reporter gene after TLR2 or TLR4 ligation were stimulated with *B. divergens* GPIs. Alkaline phosphatase activity was detected in supernatants of HEK-TLR2 cells stimulated with GPI2 to GPI9 (Fig. 5A, $p = 0.024$ Kruskal-Wallis test) and in supernatants of HEK-TLR4 cells stimulated with GPI2 to GPI10 (Fig. 5B, $p = 0.0483$ Kruskal-Wallis test) with higher activities of the last cell line, suggesting a predominant signalling through TLR4.

3.2.3. Modulation of MHC expression and apoptosis

Expression of MHC molecules has been explored on SRDC stimulated with *B. divergens* GPIs by flow cytometry after labelling with specific antibodies. No difference in MHC class I molecule expression was observed in the presence or absence of GPIs

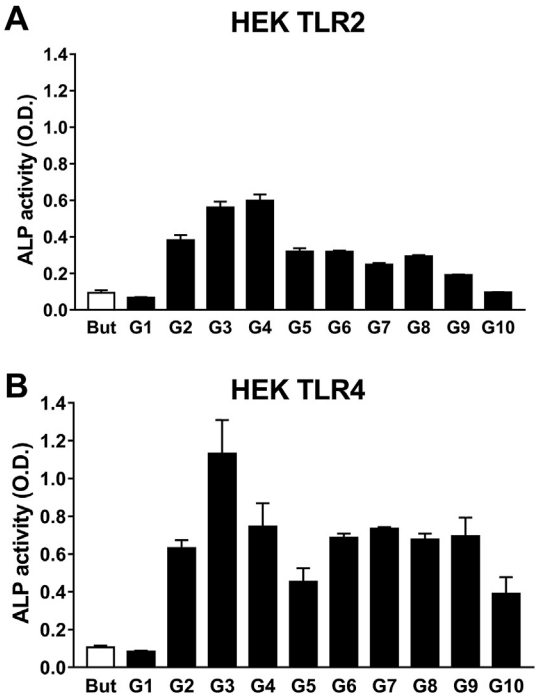

Fig. 5. TLR signalling in response to *B. divergens* GPIs. HEK-Blue™ hTLR2 (**A**) or hTLR4 (**B**) cells were stimulated for 24 h with the ten individual GPIs (G1 to G10) purified from 10^8 merozoites of *B. divergens* or with dried solvent *n*-butyl-alcohol (But) as negative control. Alkaline phosphatase activity was quantified in supernatant by addition of QUANTI-Blue™ detection medium and measurement at 630 nm. Results are mean +SEM of optical density (n = 2).

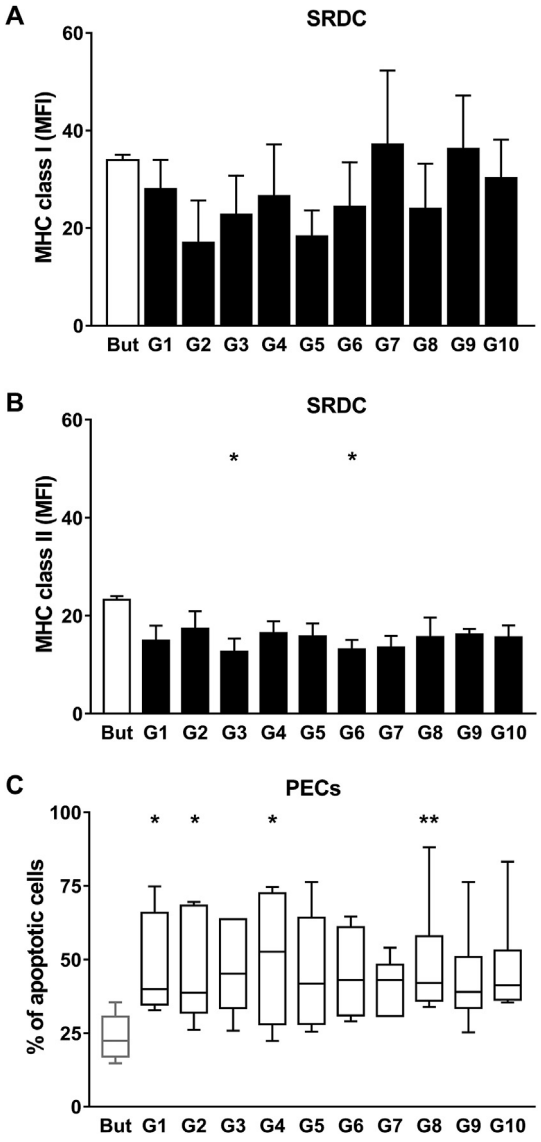

Fig. 6. MHC expression on SRDC and apoptosis of PECs in response to GPIs of *B. divergens*. SRDC (**A, B**) and PECs (**C**) cells were stimulated for 24 h with ten individual GPIs (G1 to G10) purified from 5×10^8 merozoites of *B. divergens* or with dried solvent *n*-butyl-alcohol (But) as negative control. Expression of MHC classe I (**A**) and of MHC class II (**B**) was measured at the surface of SRDC by flow cytometry after labelling with specific antibody. Results are mean +SEM of mean fluorescence intensity (MFI) (n = 4). Histograms are representative of 6 independent experiments. Apoptosis was evaluated by flow cytometry after labelling with annexin V-FITC at the surface of PECs (**C**). Each box represents results obtained with the cells from 6 different mice.

(Fig. 6A), whereas *B. divergens* GPIs decreased MHC class II molecule expression at the surface of the cells (Fig. 6B). Although the difference was significant for GPI3 and GPI6, the global statistical analysis is not significant ($p = 0.22$ Kruskal-Wallis test). Because apoptosis is difficult to evaluate in immortalized cell lines, PECs primary cells have been chosen for the study of apoptosis in response to *B. divergens* GPIs, determined by flow cytometry after labelling with annexin V-FITC. The percentage of necrotic cells (annexin V-FITC and propidium iodide double positive cells) was less than 2% in all conditions (data not shown). The percentage of apoptotic PECs (annexin V-FITC positive cells and propidium iodide negative cells) was relatively elevated in the control culture (Fig. 6C), certainly due to the culture conditions (no serum to avoid interference with GPIs). All GPIs of *B. divergens* increased the basal percentage of apoptotic cells, but not significantly ($p = 0.09$ Friedman test). Individually, apoptosis was significantly increased by GPI1, GPI2, GPI4 and GPI8 (Fig. 6C).

3.3. *Ex vivo* regulation of coagulation parameters by *B. divergens* GPIs

We finally asked us whether GPIs could regulate the coagulation system. Due to the difficulty to produce large amounts of GPIs, they were tested *ex vivo* and not administered *in vivo*. Blood was taken from rats to get enough volume of plasma and levels of fibrinogen, prothrombin time (PT) and APTT were measured after 30 min incubation with GPIs of *B. divergens*. As shown in Fig. 7A, the coagulation times reflecting the levels of fibrinogen were slightly increased in the presence of GPIs compared to the control ($p = 0.02$ Wilcoxon test), whereas PT (Fig. 7B) was not increased by the GPIs of *B. divergens* ($p = 0.06$ Wilcoxon test). APTT (Fig. 7C) was significantly increased by *B. divergens* GPIs *ex vivo* when tested with two different activators (polyphenol activator: $p = 0.002$ Wilcoxon test, kaolin activator: $p = 0.004$ Wilcoxon test). These results suggest a direct effect of GPIs on coagulation factors of the intrinsic pathway.

4. Discussion

By using metabolic labelling, ten different GPIs, including biosynthetic intermediates of *B. divergens* have been detected for the first time in parasites cultivated in erythrocytes. Only five GPIs have been detected in *B. bovis*, but the method used to visualize them after TLC (iodine vapors) was not sensitive enough to detect minor spots [21]. The GPI-profile of *P. falciparum* showed eight distinct peaks identified and all GPI species except one (Pfζ) carry a fatty acid on the inositol ring [22]. Amongst other apicomplexan

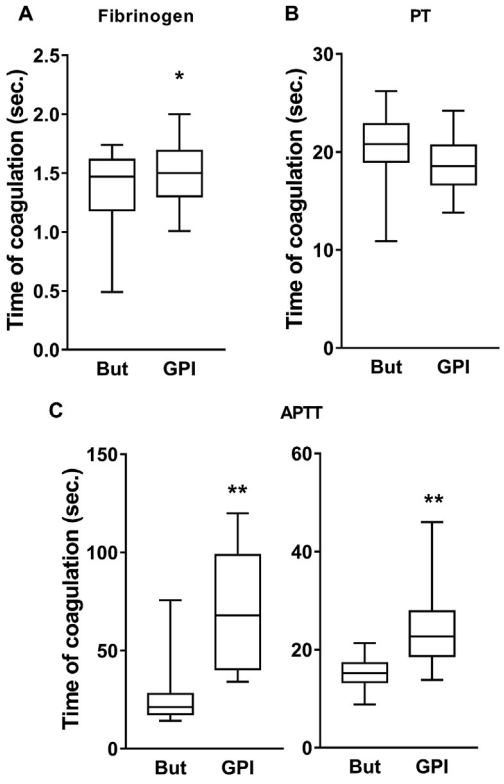

Fig. 7. Fibrinogen levels, PT and APTT coagulation parameters in response to GPIs of *B. divergens*. Rat plasma was incubated for 30 min with GPIs of *B. divergens* (from 5×10^8 merozoites for 200 µL plasma) or with the *n*-butyl alcohol solvent (But). Fibrinogen level (**A**), PT (**B**) and APTT (**C**, polyphenol activator: left histogram, kaolin activator: right histogram) are expressed in time of coagulation and given in seconds. Each box represents results obtained with the 10 different GPIs of *B. divergens*.

parasites, the GPI of the 17-kDa antigen from *Cryptosporidium parvum* contains an acylated inositol [23], whereas the inositol ring is not substituted in any of the mature GPIs of *Toxoplasma gondii* [24]. Myristic acid was the predominant modification of the inositol of GPIs purified from merozoite surface proteins-1 and -2 of the FCBR strain of *P. falciparum* [25], while palmitic acid and myristic acid represent 90% and 10%, respectively, of the acyl chain on inositol of GPIs from the FCR-3 strain of *P. falciparum* [26]. In a previous study on *B. divergens*, the GPI anchor of the Bd37 major surface antigen was identified to have a palmitic acid substitution on the inositol [27,28]. Our results confirm that palmitic acid is exclusively present on GPI4, GPI5, GPI6, GPI7 and GPI10 intermediates in *B. divergens*. In a previous work, we could find the sequences coding for only two mannosyltransferases (PIGM and PIGV, but not PIGB, the third mannosyltransferase) in the genome of *B. microti*, suggesting a di-mannose structure [28,29]. We could not rule out that one of the two mannosyltransferases or another enzyme could add a third mannose. However, a glycan structure of Man_2-GlcN has been identified in the main GPI species isolated from merozoites of *B. bovis* [21]. Here, we found the same particular structure, confirming that *Babesia* does not have the conserved GPI core glycan observed in all other eukaryotes. As no homolog of *PIGB* gene could be found in any piroplasmida genomes sequenced so far, we suggest that the presence of only two mannoses in the core glycan of the GPIs is a key feature of these parasites. Galactose is present in GPIs of *Trypanosoma* sp. and of *Entamoeba histolytica* [30,31], but this is the first time that this hexose is identified in GPIs of an *Apicomplexa*. Further analyses are needed to confirm the carbohydrate structure and to identify the final GPI anchor with ethanolamine phosphate, removed here through hydrolysis. The lipid moiety of GPI4 to GPI10 have palmitic, stearic, eicosanoic, docosanoic and tetracosanoic saturated fatty acids and oleic unsaturated fatty acid, whereas GPI1, GPI2 and GPI3 have only the longer chains (eicosanoic, docosanoic and tetracosanoic fatty acids) and no unsaturated fatty acids. In *B. bovis*, the structure of the main GPI also contains predominantly docosanoic and tetracosanoic fatty acids [21].

After infection with protozoan parasites, cells of the immune system produce Th1 cytokines playing an important role in the innate immune response and in the development of adaptive immunity. On the other hand, excess of Th1 cytokines is deleterious for the host. GPIs of *P. falciparum* have been defined as toxins eliciting hypoglycemia and excess of TNF-α production related to pyrexia and cachexia in mice [32]. GPIs of *P. falciparum* induced the production of IL-1β, TNF-α and NO by thioglycollate-elicited peritoneal macrophages [32,33]. Other studies have shown that GPIs of *T. gondii* [19,34], *T. brucei* [35] and *T. cruzi* [36] also induce Th1 cytokines (IL-12, TNF-α) by macrophages. Surprisingly, no Th1, but Th2/Th17 cytokines were secreted by antigen presenting cells stimulated by *B. divergens*. It would be interesting to expand the panel of cytokines analysed (i.e. families of IL-6 and TGF-β) to refine the profile. Studies on GPIs of *T. brucei* and *P. falciparum* have shown a dose-dependent effect on macrophages [35,37]. In the case of *T. gondii* GPIs, we have calculated that addition of individual GPI purified from 10^8 tachyzoites to a final volume of 200 µL of medium corresponds to a concentration of 1 µM [38]. Compared to LPS, 100-fold higher concentrations of *T. gondii* GPIs were required to induce similar TNF-α levels by RAW 264.7 macrophages (personal observation). Furthermore, the dose-response was not linear: around 500 pg/mL were produced with GPIs from 10^6 and 10^7 tachyzoites to jump to about 2000 pg/mL with GPIs from 10^8 and 10^9 tachyzoites, suggesting an all-or-nothing threshold to be passed for optimal cell response [34]. The same phenomenon seems to occur with *B. divergens* GPIs, since increased amounts did not lead to higher cytokine levels (data not shown).

Cytokine production was dependent on the complex *B. divergens* GPI species/target cell/cytokine. In a recent study, we have also shown that the cytokine pattern produced in response to GPIs of *N. caninum* depends on the GPI species, the type of cells (cell lines *vs*. primary cells) and the origin of the cells (murine *vs*. bovine) [39]. Thus, cells from natural host of *B. divergens* should be tested to further characterise their biological effects. Concerning the GPI structure, the present results contrast with those obtained with *T. gondii* and *P. falciparum*. Indeed, the six different *T. gondii* GPIs (GPI I to GPI VI) and the 8 different *P. falciparum* GPI species (Pfα to Pfθ) were all able to induce TNF-α production by RAW 264.7 macrophages [34,40]. However, induction of IL-5 or IL-10 production could involve different signalling pathways than TNF-α production. In *T. brucei*, it has been demonstrated that the galactose side chain of the glycosyl-inositol-phosphate (GIP) moiety is responsible for TNF-α production by macrophages [41]. *B. divergens* GPI1, with two Gal residues was unable to induce IL-5 in any cell type studied. This is maybe related to the absence of TLR2/4 signalling triggered by this GPI. However, GPI2 with one Gal residue was able to signal through TLR2/4, but also did not induce IL-5 production. TNF-α production induced by *P. falciparum* GPIs is mediated mainly through TLR2 and to a lesser extent through TLR4 [42]. On the contrary, whole GPIs of *T. gondii* activated TLR4 in the CHO cell model, but their core glycans and diacylglycerols potentially separated by macrophage phospholipases, activated both TLR2 and TLR4 in macrophages [43]. Complementary experiments are required to determine whether *B. divergens* GPIs stimulate antigen presenting cells only after their cleavage by specific enzymes. In the past, we demonstrated that GPIs not linked to proteins are

expressed at the surface of *T. gondii* tachyzoites and clustered in lipid rafts [44]. Furthermore, GPIs not linked to proteins have been detected in the culture supernatant of the apicomplexan parasite *Neospora caninum*, suggesting their secretion by the tachyzoites [39]. Both surface and secreted GPIs not linked to proteins might also exist in *B. divergens* and, via their recognition by TLRs, contribute to the global response occurring at the parasite synapse when the merozoites are released from the erythrocytes.

The fatty acid moieties could also be responsible for distinct cell responses, but GPI1 and GPI2 have same chains in very close proportions. Lipids composition is the only difference between GPI4, GPI5 and GPI6. The three species induced similar cytokine profiles, but GPI4 significantly increases apoptosis and GPI6 significantly decreased MHC class II expression. A study on the effect of GPIs on MHC expression has demonstrated that GPIs of *T. gondii* increased expression of MHC class I and II molecules at the surface of bone marrow-derived macrophages [45]. The reduction of MHC class II expression confirms the opposite effect of GPIs of *B. divergens* on antigen presenting cells. Apoptosis of non-infected cells participates in pathogenesis of diseases due to virus, bacteria, or parasites. For example, host cell exosomes containing HIV Negative Factor or Ebola VP40, caused apoptosis of bystander lymphocytes, contributing to dysregulation of the immune system and higher viral replication [46,47]. In precedent studies, we have demonstrated that GPIs of *P. falciparum* increased apoptosis of primary rat cardiomyocytes after 48-h incubation [48], whereas GPIs of *T. gondii* were not able to induce apoptosis of HL60 cells [49]. In the present work, GPIs of *B. divergens* increased apoptosis. Soluble factors secreted in culture supernatants of macrophages infected with *Mycobacterium tuberculosis* were responsible for TNF-α-independent apoptosis of bystander Jurkat T cells [50]. In another study, the 38-kDa antigen secreted by *M. tuberculosis* induced macrophage ER-stress-induced apoptosis through activation of the TLR2/4-MAPK pathway and the production of reactive oxygen species [51]. Since *B. divergens* GPIs activated TLR2/4, but did not induce TNF-α production, apoptosis of PECs might be due to ER stress.

GPIs of *B. divergens* prolonged the activated partial thromboplastin time, suggesting a direct effect of GPIs on coagulation factors of the intrinsic pathway. In the same way, GPIs of other *Babesia* species could be responsible for the increase of APTT observed *in vivo* in serum of infected animals [8]. GPIs slightly increased coagulation time when the assay used to quantify fibrinogen levels was applied. Since an increase in these levels is not possible *ex vivo*, we can only conclude that GPIs does not degrade or interfere with fibrinogen. *In vivo*, GPIs might regulate other coagulation parameters through cell activation, but this could not be evaluated here.

Altogether, our study highlighted a unique biological profile of GPIs of *B. divergens* on antigen presenting cells compared to GPIs from all other protozoan parasites studied until now. This first study lays the foundations for understanding the roles played by GPIs in inflammation and coagulation during babesiosis. Th1/Th2 balance controls the fate (survival or death) of animals and human beings infected with protozoan parasites, especially the intracellular ones. The Th2 polarization of antigen presenting cells associated with the decrease in MHC class II expression induced by the GPIs of *B. divergens* are in favour of tolerance for the pathogen. Nevertheless, other molecules from *Babesia* or from the host might act in synergy with or inhibit the GPIs, as shown for fatty acids [40,52], leading to the production of higher Th1 cytokines during babesiosis.

Financial support

This work was supported by the University of Tours, France (to IDP and FDG), the University of Montpellier, France (to SD and EC), the Deutsche Forschungsgemeinschaft, Germany, project grant SCHW 296/18-2 (to RTS), the Wellcome Trust, United Kingdom, project grant 093228 (to TKS) and the Campus France, France/Deutscher Akademischer Austauschdienst, Germany, PHC PROCOPE 24931RE (to RTS and EC). The funding source has no involvement in the conduct of the research and preparation of the article.

Author contributions

FDG, RTS and EC designed the research; FDG, TKS, SD, JS, VB and EC performed purification and biochemical studies; FDG, CD performed biological studies; TKS, SD, IDP, RTS and EC contributed to reagents/materials/analysis tools; FDG and TKS wrote the paper and all authors revised its final version.

Compliance with ethical standards

The experimental protocol, carried out in accordance with the European Union Directive (2010/63/EU), was approved by the Val-de-Loire Ethics Committee for Animal Experimentation and the French Ministry for Research (permit number: APAFIS#6649-2016090711251954-v2).

Declaration of competing interest

The authors declare that they have no conflicts of interest and no competing interests including employment, consultancies, stock ownership, honoraria, paid expert testimony, patent applications/registrations and grants or other funding in relation with the contents of this article.

Acknowledgments

We acknowledge Pr. Véronique Maupoil and Dr. Pierre Bredeloux from the CNRS ELR 7368 STIM for supplying rat blood.

References

[1] P.J. Krause, Human babesiosis, Int. J. Parasitol. 49 (2019) 165–174, https://doi.org/10.1016/j.ijpara.2018.11.007.
[2] M. Martinot, et al., Babesiosis in immunocompetent patients, Europe, Emerg. Inf. Disp. 17 (2011) 114–116, https://doi.org/10.3201/eid1701.100737.
[3] C.A. Lobo, M. Rodriguez, J.R. Cursino-Santos, *Babesia* and red cell invasion, Curr. Opin. Hematol. 19 (2012) 170–175, https://doi.org/10.1097/MOH.0b013e328352245a.
[4] C.A. Lobo, et al., *Babesia*: an emerging infectious threat in transfusion medicine, PLoS Pathog. 9 (2013), e1003387, https://doi.org/10.1371/journal.ppat.1003387.
[5] N.H. Saifee, P.J. Krause, Y. Wu, Apheresis for babesiosis: therapeutic parasite reduction or removal of harmful toxins or both? J. Clin. Apher. 31 (2016) 454–458, https://doi.org/10.1002/jca.21429.
[6] V. Asensi, et al., A fatal case of *Babesia divergens* infection in Northwestern Spain, Ticks Tick-Borne Dis. 9 (2018) 730–734, https://doi.org/10.1016/j.ttbdis.2018.02.018.
[7] R. Rafaj, et al., Alterations in some blood coagulation parameters in naturally occurring cases of canine babesiosis, Acta Vet. Hung. 57 (2009) 295–304, https://doi.org/10.1556/AVet.57.2009.2.10.
[8] ThP.M. Schetters, et al., Systemic inflammatory responses in dogs experimentally infected with *Babesia canis*; a haematological study, Vet. Parasitol. 162 (2009) 7–15, https://doi.org/10.1016/j.vetpar.2009.02.012.
[9] R.G. Bastos, et al., Differential response of splenic monocytes and DC from cattle to microbial stimulation with *Mycobacterium bovis* BCG and *Babesia bovis* merozoites, Vet. Immunol. Immunopathol. 115 (2007) 334–345, https://doi.org/10.1016/j.vetimm.2006.11.001.
[10] G. Guan, et al., Course of infection by *Babesia* sp. BQ1 (Lintan) and *B. divergens* in sheep depends on the production of IFNγ and IL10, Parasite Immunol. 32 (2010) 143–152, https://doi.org/10.1111/j.1365-3024.2009.01169.x.
[11] Y.-I. Jeong, et al., Induction of IL-10-producing $CD1d^{high}CD5^{+}$ regulatory B cells following *Babesia microti*-infection, PLoS One 7 (2012), e46553, https://doi.org/10.1371/journal.pone.0046553.
[12] A. Goddard, et al., Excessive pro-inflammatory serum cytokine concentrations in virulent canine babesiosis, PLoS One 11 (2016), e0150113, https://doi.org/10.1371/journal.pone.0150113.

[13] D. Chen, et al., Helper T cell and antibody responses to infection of CBA mice with *Babesia microti*, Parasite Immunol. 22 (2000) 81–88, https://doi.org/10.1046/j.1365-3024.2000.00279.x.
[14] R.W. Stich, et al., Stimulation of nitric oxide production in macrophages by *Babesia bovis*, Infect. Immun. 66 (1998) 4130–4136.
[15] L.K. Shoda, et al., *Babesia bovis*-stimulated macrophages express interleukin-1 beta, interleukin-12, tumor necrosis factor alpha, and nitric oxide and inhibit parasite replication in vitro, Infect. Immun. 68 (2000) 5139–5145.
[16] G. Gimenez, et al., Lipids from attenuated and virulent *Babesia bovis* strains induce differential TLR2-mediated macrophage activation, Mol. Immunol. 47 (2010) 747–755, https://doi.org/10.1016/j.molimm.2009.10.014.
[17] F. Debierre-Grockiego, R.T. Schwarz, Immunological reactions in response to apicomplexan glycosylphosphatidylinositols, Glycobiology 20 (2010) 801–811, https://doi.org/10.1093/glycob/cwq038.
[18] N. Azzouz, H. Shams-Eldin, R.T. Schwarz, Removal of phospholipid contaminants through precipitation of glycosylphosphatidylinositols, Anal. Biochem. 343 (2005) 152–158, https://doi.org/10.1016/j.ab.2005.04.030.
[19] S. Niehus, et al., Virulent and avirulent strains of *Toxoplasma gondii* which differ in their glycosylphosphatidylinositol content induce similar biological functions in macrophages, PLoS One 9 (2014) e85386, https://doi.org/10.1371/journal.pone.0085386.
[20] T.K. Smith, et al., The role of inositol acylation and inositol deacylation in the *Toxoplasma gondii* glycosylphosphatidylinositol biosynthetic pathway, J. Biol. Chem. 282 (2007) 32032–32042, https://doi.org/10.1074/jbc.M703784200.
[21] A.E. Rodríguez, et al., *Babesia bovis* contains an abundant parasite-specific protein-free glycerophosphatidylinositol and the genes predicted for its assembly, Vet. Parasitol. 167 (2010) 227–235, https://doi.org/10.1016/j.vetpar.2009.09.024.
[22] P. Gerold, A. Dieckmann-Schuppert, R.T. Schwarz, Glycosylphosphatidylinositols synthesized by asexual erythrocytic stages of the malarial parasite, *Plasmodium falciparum*. Candidates for plasmodial glycosylphosphatidylinositol membrane anchor precursors and pathogenicity factors, J. Biol. Chem. 269 (1994) 2597–2606.
[23] J.W. Priest, et al., The immunodominant 17-kDa antigen from *Cryptosporidium parvum* is glycosylphosphatidylinositol-anchored, Mol. Biochem. Parasitol. 113 (2001) 117–126.
[24] B. Striepen, et al., Molecular structure of the “low molecular weight antigen” of *Toxoplasma gondii*: a glucose alpha 1-4 N-acetylgalactosamine makes free glycosyl-phosphatidylinositols highly immunogenic, J. Mol. Biol. 266 (1997) 797–813, https://doi.org/10.1006/jmbi.1996.0806.
[25] P. Gerold, et al., Structural analysis of the glycosyl-phosphatidylinositol membrane anchor of the merozoite surface proteins-1 and -2 of *Plasmodium falciparum*, Mol. Biochem. Parasitol. 75 (1996) 131–143.
[26] R.S. Naik, et al., Glycosylphosphatidylinositol anchors of *Plasmodium falciparum*: molecular characterization and naturally elicited antibody response that may provide immunity to malaria pathogenesis, J. Exp. Med. 192 (2000) 1563–1576.
[27] S. Delbecq, et al., *Babesia divergens*: cloning and biochemical characterization of Bd37, Parasitology 125 (2002) 305–312.
[28] S. Nathaly Wieser, et al., Vaccination against babesiosis using recombinant GPI-anchored proteins, Int. J. Parasitol. 49 (2019) 175–181, https://doi.org/10.1016/j.ijpara.2018.12.002.
[29] E. Cornillot, et al., Sequencing of the smallest Apicomplexan genome from the human pathogen *Babesia microti*, Nucleic Acids Res. 40 (2012) 9102–9114, https://doi.org/10.1093/nar/gks700.
[30] M.A. Ferguson, K. Haldar, G.A. Cross, *Trypanosoma brucei* variant surface glycoprotein has a sn-1,2-dimyristyl glycerol membrane anchor at its COOH terminus, J. Biol. Chem. 260 (1985) 4963–4968.
[31] S. Moody-Haupt, et al., The major surface antigens of *Entamoeba histolytica* trophozoites are GPI-anchored proteophosphoglycans, J. Mol. Biol. 297 (2000) 409–420, https://doi.org/10.1006/jmbi.2000.3577.
[32] L. Schofield, F. Hackett, Signal transduction in host cells by a glycosylphosphatidylinositol toxin of malaria parasites, J. Exp. Med. 177 (1993) 145–153.
[33] S.D. Tachado, et al., Glycosylphosphatidylinositol toxin of *Plasmodium* induces nitric oxide synthase expression in macrophages and vascular endothelial cells by a protein tyrosine kinase-dependent and protein kinase C-dependent signaling pathway, J. Immunol. Baltim. Md 1950 156 (1996) 1897–1907.
[34] F. Debierre-Grockiego, et al., Roles of glycosylphosphatidylinositols of *Toxoplasma gondii*. Induction of tumor necrosis factor-alpha production in macrophages, J. Biol. Chem. 278 (2003) 32987–32993, https://doi.org/10.1074/jbc.M304791200.
[35] S.D. Tachado, L. Schofield, Glycosylphosphatidylinositol toxin of *Trypanosoma brucei* regulates IL-1 alpha and TNF-alpha expression in macrophages by protein tyrosine kinase mediated signal transduction, Biochem. Biophys. Res. Commun. 205 (1994) 984–991, https://doi.org/10.1006/bbrc.1994.2763.
[36] M.M. Camargo, et al., Glycosylphosphatidylinositol-anchored mucin-like glycoproteins isolated from *Trypanosoma cruzi* trypomastigotes initiate the synthesis of proinflammatory cytokines by macrophages, J. Immunol. Baltim. Md 1950 158 (1997) 5890–5901.
[37] J. Zhu, G. Krishnegowda, D.C. Gowda, Induction of proinflammatory responses in macrophages by the glycosylphosphatidylinositols of *Plasmodium falciparum*: the requirement of extracellular signal-regulated kinase, p38, c-Jun N-terminal kinase and NF-kappaB pathways for the expression of proinflammatory cytokines and nitric oxide, J. Biol. Chem. 280 (2005) 8617–8627, https://doi.org/10.1074/jbc.M413539200.
[38] F. Debierre-Grockiego, et al., Binding of *Toxoplasma gondii* glycosylphosphatidylinositols to galectin-3 is required for their recognition by macrophages, J. Biol. Chem. 285 (2010) 32744–32750, https://doi.org/10.1074/jbc.M110.137588.
[39] H. Débare, et al., In vitro cellular responses to *Neospora caninum* glycosylphosphatidylinositols depend on the host origin of antigen presenting cells, Cytokine 119 (2019) 119–128, https://doi.org/10.1016/j.cyto.2019.03.014.
[40] F. Debierre-Grockiego, et al., Fatty acids from *Plasmodium falciparum* down-regulate the toxic activity of malaria glycosylphosphatidylinositols, Infect. Immun. 74 (2006) 5487–5496, https://doi.org/10.1128/IAI.01934-05.
[41] S. Magez, et al., The glycosyl-inositol-phosphate and dimyristoylglycerol moieties of the glycosylphosphatidylinositol anchor of the trypanosome variant-specific surface glycoprotein are distinct macrophage-activating factors, J. Immunol. Baltim. Md 1950 160 (1998) 1949–1956.
[42] G. Krishnegowda, et al., Induction of proinflammatory responses in macrophages by the glycosylphosphatidylinositols of *Plasmodium falciparum*: cell signaling receptors, glycosylphosphatidylinositol (GPI) structural requirement, and regulation of GPI activity, J. Biol. Chem. 280 (2005) 8606–8616, https://doi.org/10.1074/jbc.M413541200.
[43] F. Debierre-Grockiego, et al., Activation of TLR2 and TLR4 by glycosylphosphatidylinositols derived from *Toxoplasma gondii*, J. Immunol. Baltim. Md 1950 179 (2007) 1129–1137.
[44] N. Azzouz, et al., *Toxoplasma gondii* grown in human cells uses GalNAc-containing glycosylphosphatidylinositol precursors to anchor surface antigens while the immunogenic Glc-GalNAc-containing precursors remain free at the parasite cell surface, Int. J. Biochem. Cell Biol. 38 (2006) 1914–1925, https://doi.org/10.1016/j.biocel.2006.05.006.
[45] F. Debierre-Grockiego, et al., *Toxoplasma gondii* glycosylphosphatidylinositols up-regulate major histocompatibility complex (MHC) molecule expression on primary murine macrophages, Innate Immun. 15 (2009) 25–32, https://doi.org/10.1177/1753425908099936.
[46] M. Lenassi, et al., HIV Nef is secreted in exosomes and triggers apoptosis in bystander $CD4^+$ T cells, Traffic 11 (2010) 110–122, https://doi.org/10.1111/j.1600-0854.2009.01006.x.
[47] M.L. Pleet, et al., Ebola VP40 in exosomes can cause immune cell dysfunction, Front. Microbiol. 7 (2016) 1765, https://doi.org/10.3389/fmicb.2016.01765.
[48] K. Wennicke, et al., Glycosylphosphatidylinositol-induced cardiac myocyte death might contribute to the fatal outcome of *Plasmodium falciparum* malaria, Apoptosis 13 (2008) 857–866, https://doi.org/10.1007/s10495-008-0217-6.
[49] F. Debierre-Grockiego, et al., *Toxoplasma gondii* glycosylphosphatidylinositols are not involved in *T. gondii*-induced host cell survival, Apoptosis 12 (2007) 781–790, https://doi.org/10.1007/s10495-006-0038-4.
[50] S.H.-F. Macdonald, et al., Networked T cell death following macrophage infection by *Mycobacterium tuberculosis*, PLoS ONE 7 (2012), e38488, https://doi.org/10.1371/journal.pone.0038488.
[51] Y.-J. Lim, et al., *Mycobacterium tuberculosis* 38-kDa antigen induces endoplasmic reticulum stress-mediated apoptosis via toll-like receptor 2/4, Apoptosis 20 (2015) 358–370, https://doi.org/10.1007/s10495-014-1080-2.
[52] F. Debierre-Grockiego, et al., Fatty acids isolated from *Toxoplasma gondii* reduce glycosylphosphatidylinositol-induced tumor necrosis factor alpha production through inhibition of the NF-kappaB signaling pathway, Infect. Immun. 75 (2007) 2886–2893, https://doi.org/10.1128/IAI.01431-06.